David Hellmann*
David W. Agar

Modeling of Slug Velocity and Pressure Drop in Gas-Liquid-Liquid Slug Flow

Gas-liquid-liquid slug flow in a capillary reactor is a promising new concept that allows one to incorporate gas-liquid reaction, liquid-liquid extraction, and facile catalyst separation in a single unit. In order to assess the performance of a gas-liquid-liquid slug flow reactor, it is necessary to predict the slug velocity and pressure drop to ascertain residence times and reaction rates. New empirical models for velocity and pressure drop were developed based on existing models for two-phase gas-liquid and liquid-liquid slug flows, and these were validated experimentally.

Keywords: Capillary microreactor, Gas-liquid-liquid segmented flow, Multiphase flow, Pressure calculation, Slug flow, Velocity calculation

Received: January 31, 2019; *revised:* March 27, 2019; *accepted:* July 04, 2019

DOI: 10.1002/ceat.201900087

1 Introduction

Gas-liquid-liquid slug flow is a novel operating mode for microreactors with repetitive sequences of slug triplets comprising a gas and two immiscible liquid segments flowing down a capillary. The gas and one of the liquid phases constitute the reaction medium, while the remaining liquid phase can serve as either a carrier for a catalyst or as a solvent for extraction. The use of a distinct second liquid phase facilitates separation from the reaction media following reaction, while the intense mass transfer resulting from the Taylor vortices within the individual slug ensure good mass transfer between the phases. The most stable form of slug flow for triphasic systems is that of a slug doublet comprising the gas and the dispersed or non-wetting liquid phase separated by the continuous or wetting liquid phase (Fig. 1). Other flow arrangements are possible and can be realized under the corresponding experimental conditions, but tend to be unstable and revert to the slug doublet structure after a given time.

Triphasic slug flow has been studied by different groups in the last years with a different focus on the subject. The generation of a stable and regular triphasic flow is more complicated than for a two-phase flow because the two different dispersed phases tend to interact with each other. Wang et al. [1, 2] and Rajesh and Buwa [3] studied the generation of triphasic slug flow in different contactor setups and developed correlations to predict the generated flow. Ladosz et al. [4] developed a pressure drop model for triphasic flow, which will be compared with the model presented in this study. The use of triphasic flow for extraction purposes was studied by different groups [5–7]. They discovered a stabilizing effect of the gas phase on the liquid-liquid slug flow, which allows higher liquid flow rates in triphasic slug flow. This effect enables higher throughput and an increased mass transfer coefficient due to the higher velocities. Application of triphasic flow for homogeneous reactions was performed by Önal et al. [8] and Cech et al. [9]. They used the second liquid phase for catalyst separation, in the case of gas-liquid reaction, or the improved flow stability mentioned before to achieve more favorable reaction conditions.

The ability to predict slug velocity and pressure drop for segmented gas-liquid-liquid slug flow in capillaries is critical for the design of such microreactors. Calculation of the residence time distribution and mass transfer, which are crucial for the design of the extractive and reactive processes, in turn, depend on robust modeling of the pressure drop and velocity [10]. Thus, a rapid and reliable technique for determining these quantities is essential for a further development of such reactors.

Since the pressure drop depends on the slug velocity, the latter should be established first. The first theoretical calculation of slug velocity was carried out by Bretherton [11], who derived a correlation for the thickness of the wall film formed by the wetting liquid phase based on the capillary number Ca (Eq. (1)) as given in Eq. (2) for $Ca < 5 \times 10^{-3}$ and $We < 1$.[1)]. The wall film thickness can then be used in Eq. (3) to calculate the slug velocity based on simplifying geometrical assumptions for the slug shape and the average velocity (Eq. (4)). Eqs. (1)–(3) form a closed system for ascertaining slug velocity, and therefore an iterative process must be used.

David Hellmann, Prof. David W. Agar
david.hellmann@tu-dortmund.de
Technische Universität Dortmund, Fakultät Bio- und Chemieingenieurwesen, Emil-Figge-Strasse 66, Gebäude G1 Raum 421, 44227 Dortmund, Germany.

1) List of symbols at the end of the paper.

Figure 1. Gas-liquid-liquid slug flow with the doublet slug formed by the blue aqueous phase and the white gas phase separated by the red organic phase. The slug flow is flowing from right to left, with an average velocity of 30 mm s^{-1}.

$$Ca = \frac{\eta_i u_s}{\gamma_{i,j}} \tag{1}$$

$$h = d\ 0.67\ Ca^{\frac{2}{3}} \tag{2}$$

$$u_s = \frac{2\ u_{avg}}{1 + \left(\frac{d-2\ h}{d}\right)^2} \tag{3}$$

$$u_{avg} = \frac{\dot{V}_{total}}{A} \tag{4}$$

Mac Giolla Eain et al. [12] modified the film thickness calculation for liquid-liquid systems by fitting an empirical model based on the Bretherton equation to their experimental data for the viscocapillary regime with $Ca < 0.12$ (Eq. (5)).

$$h = d\frac{0.67Ca^{\frac{2}{3}}}{1 + 2.14\ Ca^{\frac{2}{3}}} \tag{5}$$

For gas-liquid systems, Shikazono and Han [13] developed an empirical model for the film thickness (Eq. (6)), which achieved an accuracy of ± 15 % for a Ca in the range of 1.5×10^{-3} up to 2.7×10^{-1} and Reynolds numbers Re (Eq. (7)) below 2000. They incorporated a dependency on the Weber number (Eq. (8)) into their model to account for the inertial forces, as suggested by Aussillous and Quéré [14]. The influence of inertial forces is considered to be negligible in liquid-liquid systems due to the small density difference between the phases.

$$h = d\frac{0.67Ca^{\frac{2}{3}}}{1 + 3.13\ Ca^{\frac{2}{3}} + 0.504\ Ca^{0.672}\ Re^{0.589} - 0.352\ We^{0.629}} \tag{6}$$

$$Re = \frac{\rho d\ u_s}{\eta} \tag{7}$$

$$We = \frac{\rho u_s^2\ d}{\gamma} \tag{8}$$

If the resulting velocities for the gas-liquid and liquid-liquid slug flow are compared, it is apparent that the results differ (Fig. 2) and that the slug velocity for a gas-liquid-liquid system cannot be determined from the two-phase system behavior without additional information.

It can be recognized that the resulting velocity lies between the gas-liquid and liquid-liquid slug velocities. Thus, a new model is proposed (Eq. 9) that weights the film thickness of both two-phase calculations based on the phase fraction α of the dispersed phases (Eq. (10)) to determine the film thickness and, subsequently, the slug velocity for the triphasic flow.

$$h_{GLL} = \alpha^x_{slow}\ h_{slow} + \left(1 - \alpha^x_{slow}\right) h_{fast} \tag{9}$$

$$\alpha_{slow} = \frac{\dot{V}_{slow}}{\dot{V}_w + \dot{V}_g} \tag{10}$$

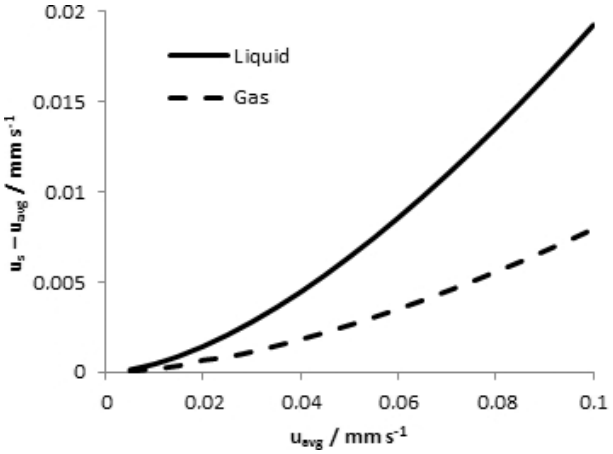

Figure 2. Theoretical results for the gas-liquid and liquid-liquid slug velocity calculated with the Bretherton model for the hexanol/water/gas system.

In some cases, no wetting film is formed, mainly due to unfavorable wetting conditions. The slug velocity is, therefore, the same as the average velocity of the multiphase flow and can be directly obtained from the volumetric flow rate and the capillary diameter.

The pressure drop in gas-liquid-liquid slug flow can be derived from gas-liquid and liquid-liquid models in a similar way, by combining and adapting the existing biphasic models, which mostly sum the pressure drop contributions of the individual phases weighted according to the volumetric fraction of the contributing phase flow and which include additional terms arising from the interfaces [15–17]. In this way, one obtains a general equation for the three-phase pressure drop (Eq. (11)), comprising the laminar pressure drop Δp_i weighted by the volumetric fraction β_i (Eq. (12)) of the corresponding phase and the term Δp_I representing the interfacial pressure drop.

$$\Delta p_{total} = \Delta p_o \beta_o + \Delta p_w \beta_w + \Delta p_g \beta_g + \Delta p_I \tag{11}$$

$$\beta_i = \frac{\dot{V}_i}{\dot{V}_{total}} \tag{12}$$

The pressure drop for laminar flow of an incompressible fluid is calculated from the Hagen-Poiseuille expression (Eq. (13)), which can be rearranged and integrated to obtain Eq. (14) [18]. The contribution of Δp_g can be assumed to be negligible because it is normally 600–1000 times smaller than the liquid phase pressure drop.

$$\frac{dV}{dt} = \frac{-\pi d^2}{128\ \eta}\frac{dp}{dt} \tag{13}$$

$$\Delta p_{\mathrm{i}} = \frac{64}{Re_{\mathrm{i}}} \left(\frac{\rho_{\mathrm{i}}}{2}\ u_{\mathrm{s}}^2\right) \frac{L}{d} \tag{14}$$

In the case of a non-wetting system, the contribution of both liquid phases can be directly calculated using the weighted Eq. (14) [17]. For wetting systems, Jovanović et al. [17] developed a model encompassing the stagnant wall film where the contribution of the liquid slug phase can be calculated with Eq. (15) when the influence of the film is taken into account. Neglecting the film velocity, which is not zero in reality, generates an insignificant error, as shown by Jovanović et al. [17]. Only for a dispersed liquid phase with a viscosity higher than the continuous phase, it may be necessary to use a more complex moving film approach, which was also developed by Jovanović et al. [17].

$$\Delta p_{\mathrm{w}} = \frac{32\ Lu_{\mathrm{s}}}{2\ d^2 - (d-2h^2)\frac{1}{\eta_{\mathrm{o}}} + (d-2h)^2\frac{1}{\eta_{\mathrm{w}}}} \tag{15}$$

For the interfacial contribution in the non-wetting system, Khasid [15] developed Eq. (16). This relationship assumes a constant contact angle for every interface, which is not generally true; therefore, the model was modified to account for different specific contact angles at each interface (Eq. (17)). In the three-phase system, gas-water, water-organic, and organic-gas interfaces exist in each gas/water/organic slug triplet.

$$\Delta p_{\mathrm{I}} = \frac{4\gamma\cos\Theta}{d} N_{\mathrm{s}} \tag{16}$$

$$\Delta p_{\mathrm{I}} = \frac{4}{d} N_{\mathrm{s}} \sum_{\mathrm{i,j}} \gamma_{\mathrm{i,j}} \cos\Theta_{\mathrm{i,j}} \tag{17}$$

In the case of a wetting system, Warnier et al. [16] developed Eq. (18) from experimental data, considering the contribution of the gas-liquid interface. For the liquid-liquid interface, Eq. (19) can be derived from the Bretherton model.

$$\Delta p_{\mathrm{I,LL}} = 14.89 \frac{Ca^{\frac{2}{3}}}{1 + 3.34 Ca^{\frac{2}{3}}} \frac{\gamma_{\mathrm{i,j}}}{d} N_{\mathrm{s}} \tag{18}$$

$$\Delta p_{\mathrm{I,GL}} = 14.89 \frac{Ca^{\frac{2}{3}}}{1 + 2.14 Ca^{\frac{2}{3}}} \frac{\gamma_{\mathrm{i,j}}}{d} N_{\mathrm{s}} \tag{19}$$

The pressure drop for a three-phase system with a wall film can, therefore, be calculated by incorporating Eqs. (12), (15), and (17)–(19) into Eq. (10). For the non-wetting system, Eqs. (12), (14), and (17) have to be used. The slug velocity used in the pressure drop calculation has to be calculated from Eq. (9) for the three-phase system with a wall film. Due to the compressibility of the gas phase, a change in capillary pressure changes the size of the gas slug, and therefore the average velocity and volumetric fractions of the triphasic system. This can be neglected for small changes, but for longer capillaries with larger pressure drop, the changes in average velocity and volume fraction have to be taken into account. The resulting equations have to be solved along the capillary using the ideal gas law to calculate the change in gas slug length. The main drawback of the scheme presented is the need to know the slug length for each phase. This has to be established from snapshots of the prevailing flow pattern, which means that the model is non-predictive. Subsequently, it is hoped to incorporate an estimate of the slug length based on the contractor geometry used and the fully developed flow conditions, or to utilize more advanced tunable coaxial contactor designs to decouple the slug length from the hydrodynamic conditions and thus gain an additional degree of freedom by setting the slug size independently. The latter option is especially helpful since the mass transfer is also highly dependent on the slug length.

The developed model is similar to the model developed by Ładosz et al. [4] but differs from it in some points. The model of Ładosz et al. [4] is a straightforward expansion of the model of Warnier et al. [16] for gas-liquid slug flow to a triphasic flow. The model does not differentiate between the wetting and the non-wetting condition in triphasic flow, which leads to large deviations between the experimental and the calculated pressure drop for the latter case. In the present model, a differentiation between the two cases is used to improve the accuracy. The model of Ładosz et al. [4] simply decreases the capillary diameter for the dispersed liquid phase by the film thickness for the laminar pressure drop and uses the model of Warnier et al. [16] for the interfacial pressure drop, which was only valid for gas-liquid cases. To improve the pressure drop calculation of the dispersed liquid phase, the model of Jovanović et al. [17] is used for the laminar contribution. An interfacial term based on the work of Mac Giolla Eain et al. [12] is used to improve the accuracy. One last difference is the use of the slug frequency instead of the slug length in the model of Ładosz et al. [4]. Since both quantities can be derived from each other, this is only a superficial difference.

2 Experimental

Hexanol, toluene, and M3 silicone oil were used as organic phases and were obtained from Sigma-Aldrich with a purity of 95 % or higher. Double-distilled water was always employed as the aqueous phase. Sudan III and methylene blue from VWR were used to dye the organic and water phases, respectively. Technical-grade nitrogen from Linde was used as the gaseous phase. All experiments were carried out in a fluorinated ethylene propylene capillary of 1 mm inner diameter within a tolerance range of ± 5 % deviation (Techlab). The three-phase flow was generated in a poly(methylmethacrylate) double T-contactor, except for the experiments involving toluene, where a poly(tetrafluoroethylene) contactor was used to ensure chemical resistance. Due to their wetting properties, hexanol and silicone oil generate a wall film and form the continuous phase. Water and gas constitute the dispersed phases being screened from contact with the capillary wall by the organic films. The toluene/water/gas system does not establish a wetting wall film; therefore, every phase is in contact with the capillary wall. Two Legato 100 syringe pumps from KD Scientific were used to generate the liquid phase flow. The gas flow was regulated with an El Flow mass flow controller from Bronkhorst.

2.1 Experimental Velocity

The velocity measurements were carried out in a straight capillary using two EE Sx1107 photosensors from Omcron Electronics, separated by a distance of 0.75 m located at 0.5 and 1.25 m along the capillary length. Flow rates of 0.5 up to 7.5 mL min^{-1} were investigated, corresponding to average velocities of 15–165 mm s^{-1}. Both signals were measured at a frequency of 600 Hz. The precision in the velocity measured should be within 2 % for the sensor setup described. To determine the change of average velocity due to gas slug expansion, the slug size was determined with a Matlab code from snapshots taken with an EDS 400D camera from Canon. At least three pictures with a minimum of 25 slugs of a given phase were used to calculate the medium slug length at the beginning and at the end of the measurement range. The maximum derivation in slug size was less than 3.5 % for silicone oil and less than 2 % for hexanol and toluene. The change in velocity is in the range of the measurement sensor and was therefore neglected. The experiments were performed with single slugs or slug doublets, respectively, under continuous flow conditions. The single-slug experiments were used to study longer slugs, which could not be realized with continuous operation, and thus to extend the range of phase ratios possible in the experiments.

The tolerance of ± 5 % in the capillary diameter exerts a noticeable effect on the velocity measured. The variation in the diameter greatly increases the experimental error to ± 10 %; therefore, the diameter of the capillary has to be determined. This was done by measuring the slug velocity for the hexanol-water and hexanol-nitrogen slug flow and by fitting the capillary diameter to achieve the best agreement with the velocities calculated from Eqs. (2), (4), and (5). The new capillary diameter of 0.98 mm thus determined is well within the 5 % tolerance range. The experimental and theoretical results for the diameter of 0.98 mm are illustrated in Fig. 3 a, b. Good agreement between the experimental and theoretical behaviors for the Bretherton model for liquid-liquid systems and gas-liquid correlations can be observed.

2.2 Experimental Pressure Drop

The pressure drop is measured with a setup similar to that for the velocity determination. The pressure is monitored at a capillary length of 0.5 and 1.5 m with two D8A-01 AirCom Pneumatics pressure sensors. The pressure difference between these two points is used for further calculations, in order to exclude the influence of slug generation. The pressure drop is measured for a velocity range of 15–165 mm s^{-1} or 0.75–7.5 mL min^{-1}.

Similar to the velocity measurements, the slug size was determined with a Matlab code from snapshots taken with an EDS 400D camera from Canon, and at least three pictures with a minimum of 25 slugs of a given phase were used to calculate the medium slug length. The contact angels were determined with the help of an IX71 fluorescence microscope from Olympus, using a manual evaluation process resulting in a relatively high uncertainty level of up to ± 7 %.

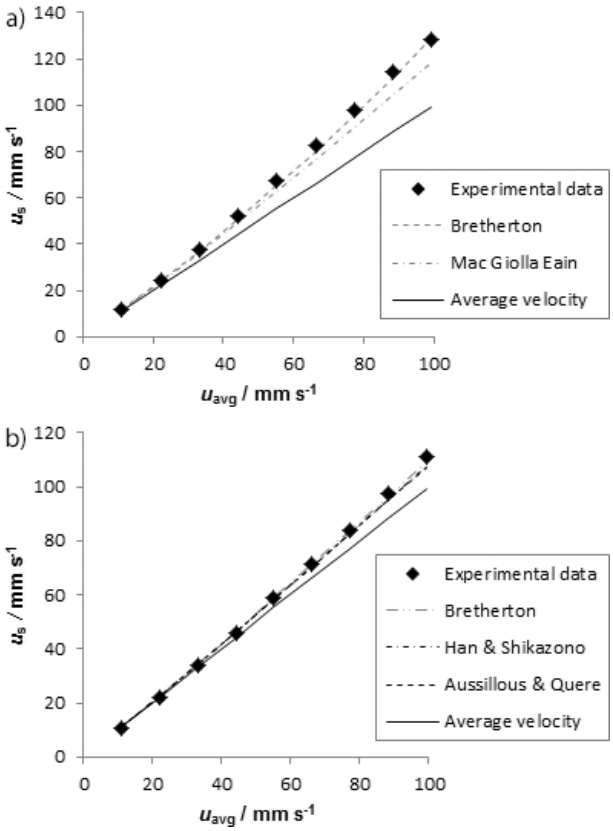

Figure 3. Experimental results for (a) the hexanol/water and (b) the hexanol/nitrogen system. The experimental data is compared to the theoretical results for a capillary with an inner diameter of 0.98 mm.

3 Results and Discussion

Fig. 4 a, b illustrates the results for the three-phase velocity measurements with hexanol and silicone oil for a gas/water phase ratio of unity and a slug length of 3 mm. The results suggest that the three-phase velocity is almost identical to the slower speed calculated for two-phase flow. Even if the capillary diameter determined is not completely correct, leading to minor errors in the calculated velocities, the similarity between the velocities measured in the two-phase and the three-phase systems is convincing. It is thus considered acceptable to ascertain the velocity of a three-phase system from the lower two-phase velocity as a first approximation for a phase ratio of 1.

To establish the effect of the gas-water slug length ratio on the doublet slug velocity, the dispersed phase ratio was varied between 0.25 and 3.0 to yield different slug lengths. The slower phase is maintained at a slug length of 3 mm in all experiments and the length of the faster phase is varied between 1 and 12 mm. The results are shown in Fig. 5 a, b, in which it can be seen that the influence of the phase ratio is small. Only for a very low phase ratio, a small increase in velocity is observed. Eq. (9) is fitted to these experimental results to obtain a value

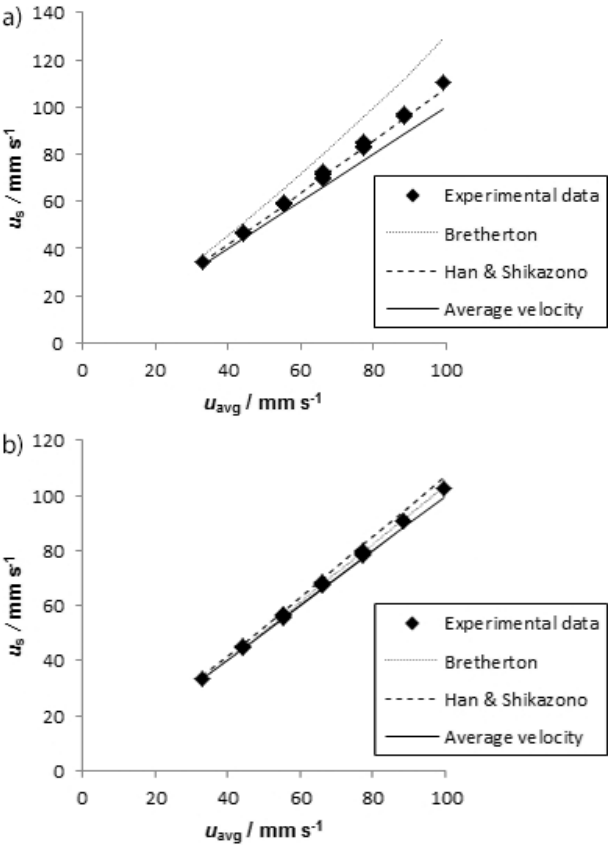

Figure 4. Comparison of experimental three-phase results for (a) hexanol-water-nitrogen and (b) silicone oil M3-water-nitrogen, with the theoretical velocities for a liquid-liquid and gas-liquid slug flow at the same volumetric flow rate.

of 0.15 for the exponential factor x. The equation describes all the experimental results well, as depicted in Fig. 5 a, b, with a relative error between the experimental results and the empirical fit calculated by Eq. (20) of 2.3 %.

$$F = \frac{1}{N_{exp}} \sum_{n=1}^{N_{exp}} \left| \frac{X_{exp} - X_{emp}}{X_{exp}} \right| \tag{20}$$

To determine the influence of the contactor on the overall pressure drop, the differential pressure drop between the two sensors and the pressure of the second sensor at 1.5 m and the pressure in the gas feed upstream of the contactor were compared. The results illustrated in Fig. 6 indicate that the pressure drop in the capillary is significantly higher than that of the contactor, which can thus be neglected in the overall pressure drop determination. The influence of the contactor will further diminish when the length of the capillary is increased.

The results for the pressure drop calculation are shown in Fig. 7. All the experimental results for silicone oil and hexanol lay within ± 20 % of the empirical correlation, which is considered adequate for a pressure drop estimation. The average relative error between experiment and model is 16.6 %. Pressure drop prediction for three-phase systems with a wall film is thus feasible and comparable to the results of Ładosz et al. [4] which also lay within ± 20 %. The results presented in Fig. 7 were calculated without considering the change in gas slug caused by the pressure drop. A more complex approach, where the volumetric fractions and the gas slug length were recalculated every 10 cm, was tested but does not significantly increase the accuracy of the results. This is due to counteracting effects of different parts in the pressure drop equation. While the laminar pressure drop and the interfacial pressure drop increase with increasing velocity, the number of interfaces per meter decreases. Additionally, the gas fraction, which has a significantly lower pressure drop per meter compared to the liquid fractions, increases as well. Nevertheless, the pressure drop for an unknown system should always be calculated with changing average velocity and phase fraction to achieve the best estimation.

The deviation for the non-wetting toluene/gas/water system, which does not form a wall film, is sometimes substantially higher than 20 %. It is obvious that the pressure drop is underestimated in most cases and that the accuracy of the estimation is increasing with the overall pressure drop and velocity, which was also observed by Ładosz et al. [4]. Compared to Ładosz et al. [4], the presented results are more accurate, with the estimated pressure drop being in the range of 30 to 100 % of the experimental results, where the results of Ładosz et al. [4] are below 40 %. The changed term for the interfacial pressure drop is, therefore, increasing the accuracy of the estimation, but not to a satisfacional level.

To increase the accuracy, it is necessary to perform a more detailed study of the problem. The presented model combines the pressure drop of a laminar flow with the pressure drop over a curved surface, which should theoretically describe the complete pressure drop, but the constant underprediction of the pressure drop indicates that an additional pressure drop contribution is missing. This additional pressure drop has to be linked in some way to the movement of the interfaces, as the effect of the stagnant interface and the laminar flow are present in the model.

Additionally, the accuracy of the dynamic contact angle determination has to be increased. The uncertainty in this study was quite high in some cases and the influence of the interfaces on the overall pressure drop is high. For example, the interfacial pressure drop for a triphasic toluene flow with 3 mm slug length and equal volume fractions is 4.9 times higher than the laminar pressure drop for an average of 15 mm s^{-1}, this ratio decreases to 1.3 for 100 mm s^{-1}. It is, therefore, necessary to improve the contact angle determination for three-phase systems without film. This is, however, a challenging task. The contact angle is neither always constant along the capillary nor axisymmetric, and it is influenced by minimal changes of the surface properties. The most preferable option would be to determine the dynamic contact angle with a correlation based on flow properties and the static contact angle. This would eliminate the need for microscopic images from the actual flow and therefore reduce the experimental effort for the pressure drop determination.

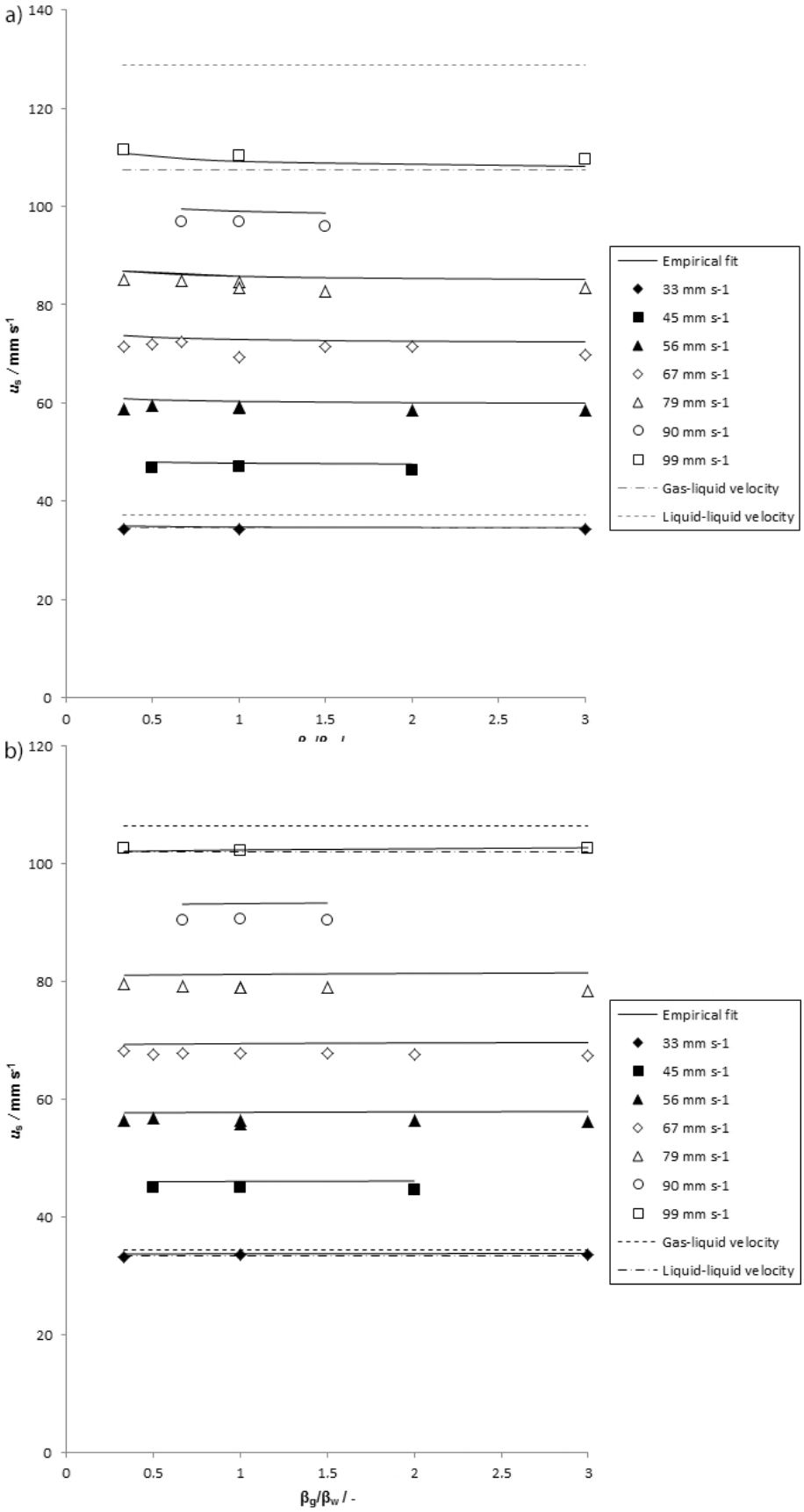

Figure 5. Experimental data and empirical fit for three-phase slug flow of (a) hexanol-water-gas and (b) silicone oil M3-water-gas for different ratios of the dispersed phases and different average velocities. The continuous lines denote the empirical fit and the dashed lines show the gas-liquid and liquid-liquid velocity for the fastest and slowest velocity found for comparison with the three-phase slug flow.

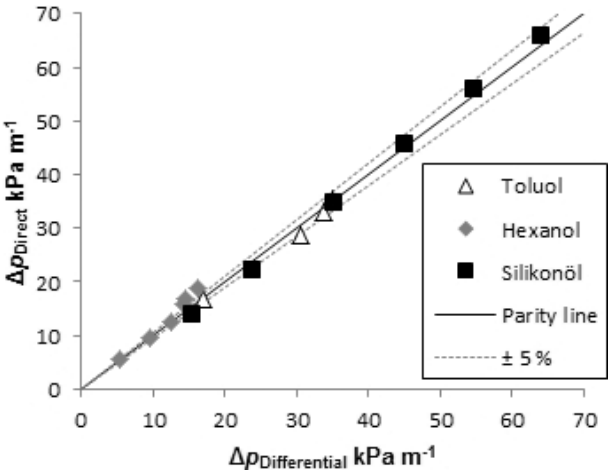

Figure 6. Measured direct and differential pressure drops for three-phase slug flow with toluene, hexanol and silicone oil for total volumetric flow rates between 0.75 and 7.5 mL min^{-1}.

4 Summary

Based on the empirical models for two-phase slug velocity and pressure drop, new models for three-phase gas-liquid-liquid slug flow were developed and experimentally verified. The velocities can be predicted with a high degree of accuracy with the new models, which are valid over a wide range of velocities and gas-liquid phase ratios. Pressure drop prediction is possible with an error of less than 20 % for wetting systems with a wall film. To enhance the precision of pressure drop estimation for non-wetting systems, it is considered necessary to improve the contact angle measurement.

The authors have declared no conflict of interest.

Symbols used

A	[m^2]	area
Ca	[–]	capillary number
d	[m]	diameter
F	[–]	relative error
g	[m s^{-2}]	gravitational force
h	[m]	height of the film
L	[m]	length
N	[–]	number
p	[Pa]	pressure
Re	[–]	Reynolds number
t	[s]	time
u	[m s^{-1}]	velocity
We	[–]	Weber number

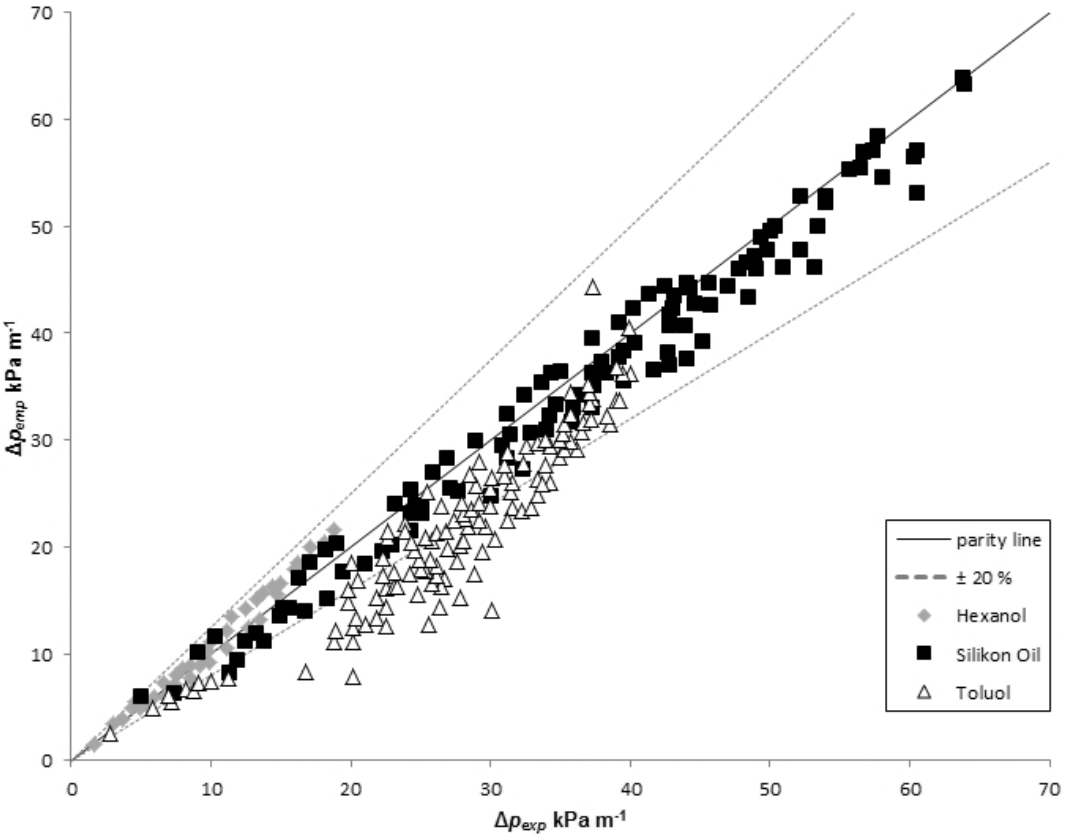

Figure 7. Comparison of experimental and empirically calculated pressure drops for three-phase slug flow with various organic solvents. The hexanol and silicone oil systems form a continuous wall film on the capillary surface. The toluene system is non-wetting and, thus, no wall film is present.

x	[–]	exponential factor
X	[variable]	compared unit

Greek symbols

α	[–]	dispersed phase fraction
β	[–]	volumetric fraction
γ	[N m^{-1}]	interfacial tension
η	[Pa s]	dynamic viscosity
Δp	[Pa m^{-1}]	pressure difference
Θ	[–]	angle

Sub-/superscripts

avg	average
emp	empirical
exp	experimental
fast	fast dispersed phase
GL	gas-liquid
GLL	gas-liquid-liquid
i	control variable
I	interface
j	control variable
LL	liquid-liquid
o	organic
s	slug
slow	slow dispersed phase
w	water

References

[1] K. Wang, Y. C. Lu, K. Qin, G. Luo, T. Wang, *Chem. Eng. Technol.* **2013**, *36 (6)*, 1047–1060. DOI: https://doi.org/10.1002/ceat.201200561

[2] K. Wang, Y. C. Lu, J. Tan, B. D. Yang, G. S. Luo, *Microfluid. Nanofluid.* **2010**, *8*, 813–821. DOI: https://doi.org/10.1007/s10404-009-0514-6

[3] V. M. Rajesh, V. V. Buwa, *Chem. Eng. J.* **2012**, *207/208*, 832–844. DOI: https://doi.org/10.1016/j.cej.2012.07.082

[4] A. Ładosz, E. Rigger, P. R. von Rohr, *Microfluid. Nanofluid.* **2016**, *20*, 49. DOI: https://doi.org/10.1007/s10404-016-1712-7

[5] N. Assmann, P. R. von Rohr, *Chem. Eng. Process.* **2011**, *50*, 822–827. DOI: https://doi.org/10.1016/j.cep.2011.05.009

[6] N. Aoki, R. Ando, K. Mae, *Ind. Eng. Chem. Res.* **2011**, *50*, 4672–4677. DOI: https://doi.org/10.1021/ie1024326

[7] Y. Su, *AlChE J.* **2009**, *55 (8)*, 1948–1958. DOI: https://doi.org/10.1002/aic.11787

[8] Y. Önal, M. Lucas, P. Claus, *Chem. Eng. Technol.* **2005**, *28 (9)*, 972–978. DOI: https://doi.org/10.1002/ceat.200500147

[9] J. Cech, M. Pribyl, D. Snita, *Biomicrofluidics* **2013**, *7 (5)*, 54103. DOI: https://doi.org/10.1063/1.4821168

[10] *Technische Chemie* (Eds: M. Baerns, A. Behr, A. Brehm, J. Gmehling, H. Hofmann, U. Onken, A. Renken), Wiley-VCH, Weinheim **2006**.

[11] F. P. Bretherton, *J. Fluid Mech.* **1961**, *10 (2)*, 166–188. DOI: https://doi.org/10.1017/S0022112061000160

[12] M. Mac Giolla Eain, V. Egan, J. Punch, *Int. J. Heat Fluid Flow* **2013**, *44*, 515–523. DOI: https://doi.org/10.1016/j.ijheatfluidflow.2013.08.009

[13] N. Shikazono, Y. Han, in *Proc. of the 7th Int. Conf. on Nanochannels, Microchannels and Minichannels*, Pohang **2009**, 1387–1394.

[14] P. Aussillous, D. Quéré, *Phys. Fluids* **2000**, *12 (10)*, 2367–2371. DOI: https://doi.org/10.1063/1.1289396

[15] M. N. Kashid, Experimental and modelling studies in liquid-liquid slug flow capillary microreactors, *Ph.D. Thesis*, Technische Univeristät Dortmund, Dortmund **2007**.

[16] M. J. F. Warnier, M. H. J. M. de Croon, E. V. Rebrov, J. C. Schouten, *Microfluid. Nanofluid.* **2010**, *8*, 33–45. DOI: https://doi.org/10.1007/s10404-009-0448-z

[17] J. Jovanović, W. Zhou, E. V. Rebrov, T. A. Nijhuis, V. Hessel, J. C. Schouten, *Chem. Eng. Sci.* **2011**, *66 (1)*, 42–54. DOI: https://doi.org/10.1016/j.ces.2010.09.040

[18] *Grundzüge der Strömungslehre*, 9th ed. (Eds: J. Zierep, K. Bühler), Springer Verlag, Wiesbaden **2013**.

